Epitaxial Growth, Processing and Characterization of Semiconductor Nanostructures

Borgström, Magnus

2003

Available online at www.sciencedirect.com
SCIENCE DIRECT®
ELSEVIER
Journal of Crystal Growth 248 (2003) 310–316
JOURNAL OF CRYSTAL GROWTH
www.elsevier.com/locate/jcrysgro

Site control of InAs quantum dots on a patterned InP surface: As/P exchange reactions

M. Borgstrom*, T. Bryllert, T. Sass[1], L.-E. Wernersson, L. Samuelson, W. Seifert

Solid State Physics, University of Lund, Box 118, Lund S-221 00, Sweden

Abstract

In this paper, we present the effect of annealing temperature and annealing time on InAs site-controlled quantum dot growth. Individual InAs quantum dots formed by self-assembling have been positioned into holes, created by partial overgrowth of electron beam induced nano-carbon deposits by metal organic vapor phase epitaxy. As/P exchange reactions produce material sufficient for selective dot nucleation in the holes. Results, showing that As/P exchange reactions occur even when capping the dots with InP are presented.

PACS: 68.55.Jk; 71.55.Eq; 73.40.Gk; 73.61.−r

Keywords: A1. Nanostructures; A3. Metalorganic vapor phase epitaxy; B1. Nanomaterials; B2. Semiconducting III–V materials

1. Introduction

Spontaneously formed quantum dots (QDs), as represented by the Stranski-Krastanow growth mode, have been studied extensively since they show a high crystalline quality that is sufficient for device applications. In the present materials system, resonant tunnelling through stacked QDs, showing extremely narrow peaks with high peak-to-valley ratios in the current–voltage characteristics has been observed recently [1]. In a previous paper, we proposed the realization of a resonant tunnelling diode based on site-controlled InAs QDs in InP, where a large InP barrier restricts current flow to the active dots only [2]. For such structures, there is a need to overcome the randomness in dot nucleation exhibited by self-organizing approaches.

The driving forces for selective area growth are local gradients in the chemical potential, which for a thin film can be written as $\mu(x,y,z=0)=\mu_0+\gamma\Omega\kappa(x,y)+\Omega E_s(x,y)$ [3], where μ_0 is the chemical potential for an unstressed surface of the bulk crystal. The second term, $\gamma\Omega\kappa(x,y)$, comes from the contribution of surface curvature, γ is the orientation dependent surface free energy, Ω is the atomic volume of the species and $\kappa(x,y)$ is the surface curvature. The third term is from the tangential stress contribution where $E_s(x,y)$ is the local strain energy on the surface. Hence, gradients in the chemical potential can be obtained either by patterning of the substrate (curvature

*Corresponding author. Tel.: +46-2227671; fax: +46-2223637.
E-mail address: magnus.borgstrom@ftf.lth.se (M. Borgstrom).
[1]Current address: OSRAM Opto Semiconductors GmbH. Wernerwerkstrasse 2, D-93049 Regensburg, Germany.

0022-0248/03/$ - see front matter
PII: S0022-0248(02)01817-1

contribution) or by creating local strain fields (strain contribution), causing a diffusion of material towards areas with lower chemical potential.

Laterally controlled dot formation by the use of lithographically defined surface pattern has been reported [4–9], and recently laterally controlled quantum dot growth that does not include the use of lithography and etching was presented [10,11].

We already previously studied the selective growth of InAs QDs in nano-holes at the surface, formed by the use of electron beam induced carbon deposits as growth masks [11]. We found that InAs dots were formed in the holes by only annealing of the surface in an arsine ambient.

In this paper, we report on the effect of annealing temperature and annealing time of the InP surface under an arsine-containing ambient on selective dot formation. Furthermore, we study the effect of capping randomly distributed InAs QDs with InP. We find that more excess InAs is formed by As/P exchange reactions even when capping the dots with InP.

2. Experimental procedure

The samples were grown by low-pressure (50 mbar) metal organic vapor phase epitaxy (MOVPE), using phosphine (PH_3), arsine (AsH_3), and trimethyl-indium (TMI) as precursors and hydrogen as carrier gas. The process was controlled by a flow and pressure balanced vent/run system. The molar fractions were 5×10^{-4} for arsine and 1.5×10^{-2} for phosphine. The total gas flow in the reactor cell was about 6000 cm^3/min. We used Sn-doped (n^+) InP (0 0 1) (''epi-ready'' Sumitomo) wafers with a 0.2° misorientation towards the nearest $\langle 0\,1\,1 \rangle$ direction for our experiments. A base structure consisting of InP(substrate)/GaInAs(300 nm)/InP(5 nm) was initially grown at an elevated temperature of 600°C. The carbon growth masks were deposited on the surface by means of an ordinary electron beam lithography system (JEOL). The focused electron beam cracks hydrocarbon molecules that derive from the oil to the vacuum pump, which deposit on the surface [12]. We used an acceleration voltage of 35 kV, a probe current of 20 pA, and a pressure in the scanning electron microscope of about 5×10^{-5} Pa. The carbon pattern was formed by irradiating a mesh of 50×50 pixels on the surface for 100 ms/pixel, forming as many nano-growth masks of about 20 nm in height and 50 nm in width [11]. The distance between the deposits was varied. The samples, with the pattern of carbon, were treated with O-plasma for 15 s at 10 mbar in order to remove the thin carbon-containing surface layer around the carbon deposit, formed by electron back scattering. The samples were then treated with diluted sulphuric acid (H_2SO_4:H_2O, 1:100) for 30 s and finally rinsed in de-ionized water, followed by 25 nm InP growth, after which the partially overgrown carbon deposits were removed completely by oxygen plasma treatment for 2 min at 5 mbar. The surfaces were inspected by means of conventional contact mode AFM. A $70 \times 70\,\mu m^2$ scanner was used to find the patterns on our samples, which were then zoomed in for closer inspection. After the first growth step, well-defined holes, elongated in $\langle 1\,1\,0 \rangle$ were observed [5]. This patterned InP surface was treated with diluted sulphuric acid and then rinsed in de-ionized water. Then the second MOVPE overgrowth step followed, in order to deposit the dots site selectively at the positions where the carbon deposits were before. The samples were heated to 630°C for 7 min under phosphine flow, before cooling down to the intended annealing temperature during a 5 min period: 500°C, 520°C or 540°C. The temperature was stabilized for 1 min before annealing of the surface under arsine for 30 s, 1 or 3 min. During this arsine annealing process, dots were preferably formed inside the holes.

For non-site-controlled dot formation, used in the capping experiments, 0.3 ML InAs was grown on the same base structure, InP/GaInAs/InP, and then the surface was annealed for 12 s under arsine pressure. Now the sample was either cooled down under arsine ambient (non-capped dots) or overgrown with 15 nm InP, followed by another 0.3 ML InAs deposition and 12 s arsine annealing of the surface (capped dots), which was then overgrown by 12 nm InP and capped with GaInAs. More details of the latter structure, with stacked QDs, can be found elsewhere [1].

3. Results and discussion

Fig. 1(a) presents a patterned InP surface onto which 0.3 ML InAs has been deposited. A few dots are observed on the planar surface, whereas many dots are found in the patterned area, inside the holes and at the side facets of the holes. In the middle of some of the holes, one large dot can be seen. Note that we reach a critical wetting layer thickness of the dot material by a deposition of only 0.3 ML. In the switching procedure for dot growth, we first switch to arsine flow for 1 s, during which 1 ML InAs is formed by materials conversion of the upper InP surface layer.

In the second step, where 0.3 ML InAs is deposited, a critical wetting layer thickness for dot formation can be reached locally. When capping the dots with InP, even more InAs may be formed by As_x incorporation from the background in the reactor cell. Fig. 1(b) shows an AFM image of an InP surface, which has been annealed for 30 s under AsH_3 pressure only. Dots formed by material from As/P exchange reactions are found in the holes, but not on the planar surface. A high sensitivity of the dot density to the available material should be noted. A critical wetting layer thickness is reached faster in the hole than on the planar surface, the material coming from local As/P conversion plus material that diffuses into the hole.

In the following, parameters for optimizing the ratio of filled/empty holes will be considered, i.e., growth temperature and annealing time. Fig. 2 shows that an increase of the annealing temperature affects the As/P exchange reactions, and thereby the dot density. At 500°C, dots are observed in some of the holes (Fig. 1(b)), at 520°C the ratio of empty/filled holes has increased (Fig. 2(a)) and at 540°C there is one dot in almost every hole (Fig. 2(b)). At the highest experimental temperature, 540°C, a few dots can even be observed on the planar surface, i.e., a higher temperature leads to relatively stronger As/P exchange reactions. Thus, we have a tool to control the density of dots formed in the holes. The facets that develop in the holes limit the density of holes that can be used without the holes merging together. With our observed facet angles (11°) and InP thickness, 25 nm, the minimum distance would be about 260 nm, corresponding to a hole (dot) density of $1.5 \times 10^9\,cm^{-2}$.

Unfortunately, no PL from the dots could be detected, due to the low overall density of dots. However, Fig. 2(c) gives some indication of the dot size found in the holes. An AFM surface line scan shows a hole, within which a dot of 8 nm in height (measured from the bottom left to the top of the dot) has nucleated. The base of the dot seems to originate in the interface between the side facet of the hole and the bottom (0 0 1) plane. Common sizes of the dots in the holes were 6–8 nm in height. Due to the design of the observed structures, AFM tip effects may influence these values.

In Fig. 3 the effect of varying the annealing time is presented, for a growth temperature of 500°C. As the annealing time is increased to 1 or 3 min, no

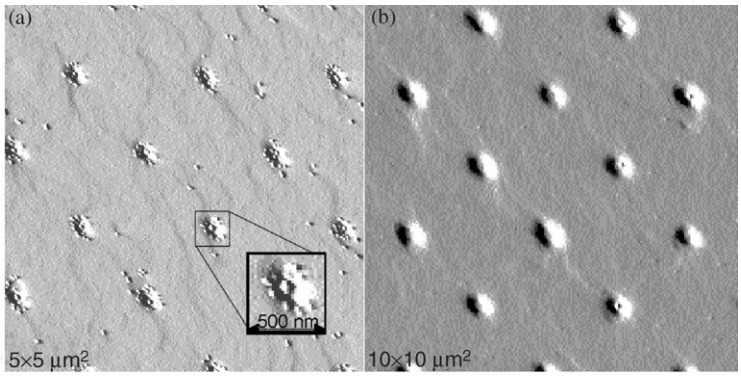

Fig. 1. Patterned surface with (a) 0.3 ML InAs + 12 s AsH_3 annealing, a magnification of one of the holes, with dots, in the figure is shown for clarity. (b) No InAs deposition 30 s AsH_3 annealing only, $T = 500$°C, AFM images are shaded from the right.

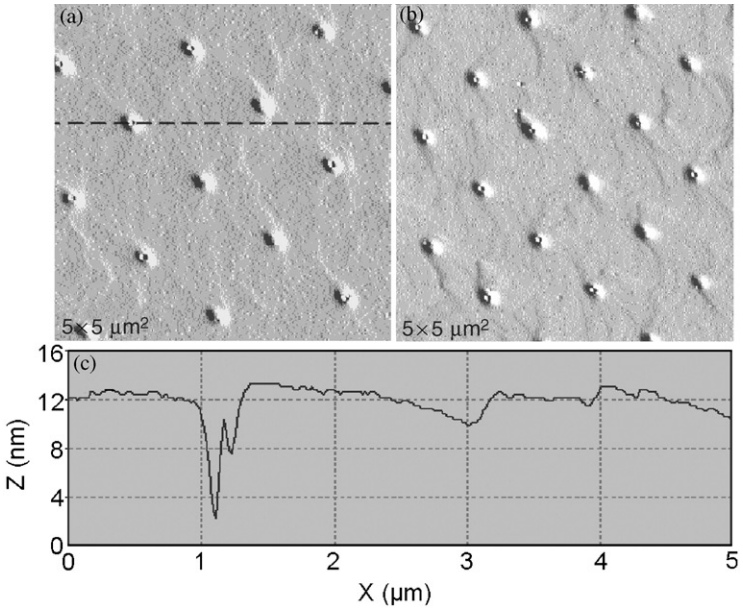

Fig. 2. Patterned surface annealed for 30 s under AsH_3 ambient at (a) 520°C, (b) 540°C, AFM images shaded from the right, (c) AFM line scan of the surface, as indicated in Fig. 2(a).

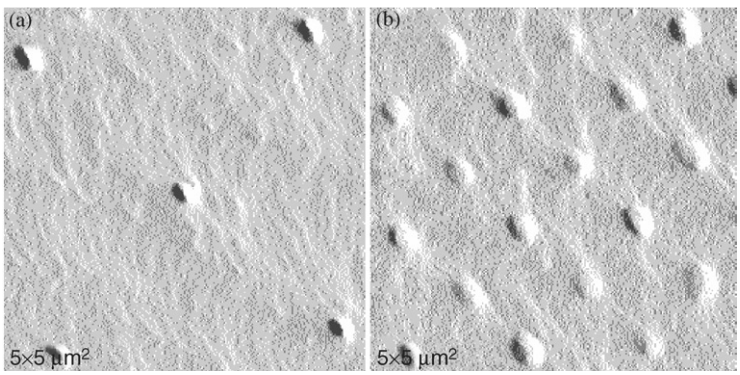

Fig. 3. Patterned InP surface annealed under AsH_3 at 500°C for (a) 1 min, (b) 3 min, AFM images are shaded from the right.

dots in the holes can be observed. It seems that a planarization of the surface occurs, indicating an alloying effect. When the annealing time is increased, mobile In species can diffuse on the surface to be incorporated at favorable nucleation sites with low chemical potential: the surface planarizes. InAs is produced at the same time as the surface is given time to reconstruct. Intermixing (alloying) reduces the local misfit, Δa, and the dots may even disappear [13]. It is likely that InAs rich clusters can be found in the holes beneath the planarized surface. In Fig. 4, the schematics of As/P exchange reactions and surface diffusion of material into a hole is shown.

The distance between the holes was then varied, 300 nm was the minimum and 5 μm the maximum distance between the holes. No effect on dot nucleation inside the patterned area of this variation was observed. Hence, we believe that most of the material contributing to dot formation

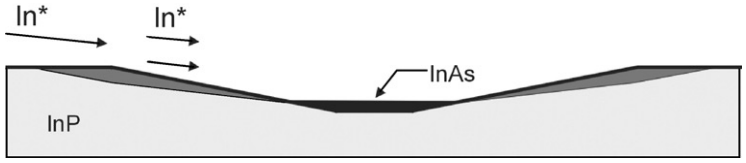

Fig. 4. Schematics of diffusion into a hole, dark regions correspond to material that converts to InAs by As/P exchange reactions and contributes to the amount of material available for dot formation.

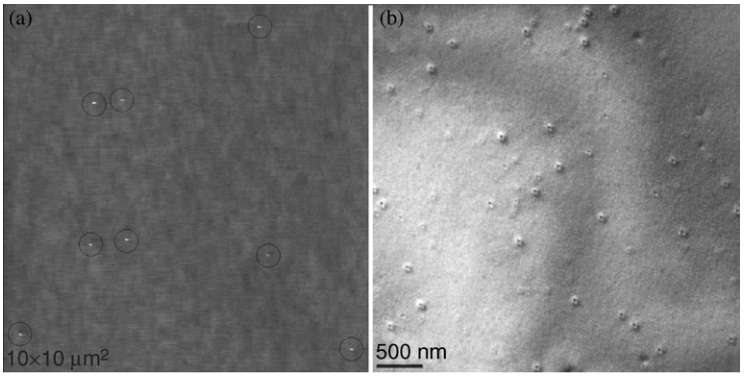

Fig. 5. Low-density InAs QD samples (a) 0.3 ML InAs deposition + 12 s AsH_3 anneal, $10 \times 10\,\mu m^2$ AFM image, dots are encircled for clarity (b) two-dot stacks 2×0.3 ML InAs separated by 15 nm InP and capped by 12 nm InP, plan-view TEM image.

is formed by consuming material from the inside of the holes and from the immediate surroundings of the holes (Fig. 4).

Since the materials system is as sensitive to As/P exchange reactions, it is of importance to study the effect of capping the dots with InP. In the following, non-site-controlled (randomly distributed) dots are used for this purpose. Fig. 5(a) shows an AFM image of the InP surface after 0.3 ML InAs deposition and 12 s annealing and then cooling down under arsine. Due to a low density of dots and the fact that the SK-dot density is so sensitive to the amount of deposited material, the dot density can vary somewhat on the sample. However, an average density of $8 \times 10^6\,cm^{-2}$ with heights of about 7 nm was observed on this sample by AFM. When capping such a structure with InP and a subsequent dot layer, the density of stacks cannot be higher than the seed dot density. Fig. 5(b) is a TEM plan-view image of a sample with two-dot stacks. Single dots, in either the first or the second InAs layer, show smaller contrast than stacked dots in the TEM image. The density of stacked dots is $2 \times 10^8\,cm^{-2}$ with heights of about 6 nm, and the total density of dots, $d_{tot} = d_{stack} + d_{single}$, is $4 \times 10^8\,cm^{-2}$. Obviously, the density of dots in the sample with capped dots is dramatically higher as compared to the density of the freestanding dots, i.e., additional dots must have been formed during capping of the dots. Complementary cross-sectional TEM images of 0.3 ML InAs embedded in InP barriers revealed an InAs wetting layer thickness of 2 ML [2]. If we assume a constant wetting layer thickness of 2 ML for InAs/InP samples and approximate the dot shape with the cap of a hemisphere, then the observed increase in dot density corresponds to another 0.1 ML InAs, formed during capping of the dots.

Electrical measurements were carried out on the capped dot structure, complementary to the TEM measurements, to verify that the overall density of stacks is really higher than the density of freestanding dots as observed by AFM. In Fig. 6, resonant tunnelling through ensembles of dots can be seen; the contact size determines how many

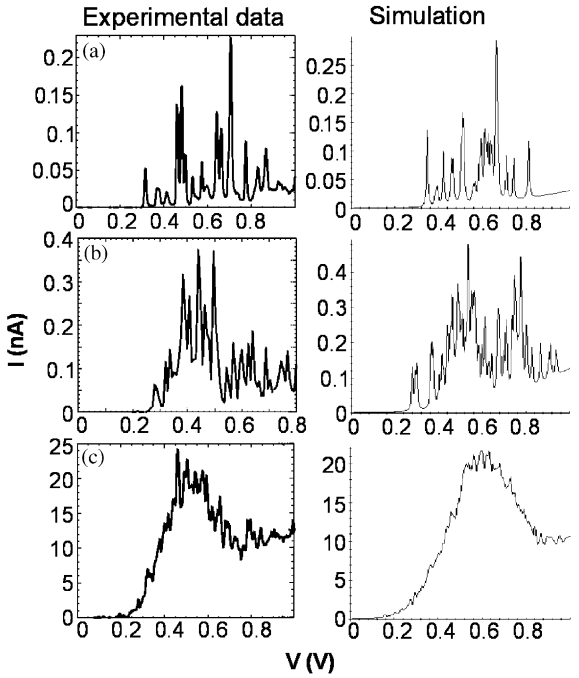

Fig. 6. Experimental and simulated results of resonant tunneling through InAs/InP two-dot stacks, contact sizes of (a) $5 \times 5\,\mu m^2$, (b) $10 \times 10\,\mu m^2$, (c) $90 \times 90\,\mu m^2$, $T = 4.2\,K$.

stacks that can exist beneath the contacts, of sizes 5, 10 and $90\,\mu m^2$. When a bias voltage is slowly increased over the sample, the discrete energy states of the dots will gradually be forced into resonance with the emitter levels, at the same time as the ground states of the two dots align. Every stack contributes to the tunnelling current with one discrete tunnelling event, or peak [14]. Tunnelling occurs at different bias for each peak and depends on the size difference of the first and the second dot in the stack, since the size influences the ground state energies. The results of simple modelling where single-stack-tunnelling peaks are randomly generated within a normal distribution centered at a bias of 0.6 V with a standard deviation of 0.15 V can be seen in Fig. 6. The peak heights depend mainly on the middle InP barrier thickness, and are considered to be randomly distributed within a normal distribution centered around 80 pA with a standard deviation of 25 pA. An exponential background has also been added to the simulation. This background is scaled with the contact area. The simulation reproduces the experimental data to a high accuracy, both in visual appearance and current flow levels. The number of tunnelling contributions is, 25, 100 and 8100 for the differently sized contacts and correspond to a dot stack density of $1 \times 10^8\,cm^{-2}$, which confirms that the density of capped dots are indeed higher than that observed from freestanding dots. We conclude that As/P exchange reactions contribute to form more material when capping the dots, and that the density of capped dots is generally higher than that of the freestanding.

In summary, carbon was deposited on an InP/GaInAs based heterostructure by means of electron beam irradiation, and was successfully used as a nano-growth mask. High selectivity of InAs dot nucleation was observed within the holes at the surface after partial overgrowth and subsequent removal of the growth masks. The influence on As/P exchange reactions by annealing temperature and annealing time was investigated. One dot per hole and no dots outside the holes could be achieved to a high degree by annealing the surface under arsine, the material for dot formation produced by As/P exchange reactions only. The dots in the holes are potential seed dots for vertical stacking experiments. We showed that As/P exchange reactions produce additional material for dot formation when the dots are capped with InP.

Acknowledgements

This work was carried out within the Nanometer Structure Consortium in Lund and was supported by grants from the Swedish Natural Science Research Council (NFR), the Swedish Research Council for Engineering Sciences (TFR) and the Swedish Foundation for Strategic Research (SSF).

References

[1] M. Borgstrom, T. Bryllert, T. Sass, B. Gustafson, L.-E. Wernersson, W. Seifert, L. Samuelson, Appl. Phys. Lett. 78 (2001) 3232.

[2] M. Borgstrom, T. Bryllert, B. Gustafson, J. Johansson, T. Sass, L.-E. Wernersson, W. Seifert, L. Samuelson, J. Electron. Mater. 30 (2001) 482.
[3] D.J. Srolovitz, Acta. Metall. 37 (1988) 621.
[4] W. Seifert, N. Carlsson, A. Petersson, L.-E. Wernersson, L. Samuelson, Appl. Phys. Lett. 68 (1996) 1684.
[5] S. Jeppesen, M. Miller, D. Hessman, B. Kowalski, I. Maximov, L. Samuelson, Appl. Phys. Lett. 68 (1996) 2228.
[6] E. Kuramochi, J. Temmyo, T. Tamamura, H. Kamada, Appl. Phys. Lett. 71 (1997) 1655.
[7] A. Konkhar, A. Madhukar, P. Chen, Appl. Phys. Lett. 72 (1998) 220.
[8] R. Zhang, R. Tsui, K. Shiralagi, D. Convey, H. Goronkin, Appl. Phys. Lett. 73 (1998) 505.
[9] G. Jin, J.L. Liu, K.L. Wang, Appl. Phys. Lett. 76 (2000) 3591.
[10] S. Kohmoto, H. Nakamura, T. Ishikawa, K. Asakawa, Appl. Phys. Lett. 75 (1999) 3488.
[11] M. Borgstrom, J. Johansson, W. Seifert, L. Samuelson, Appl. Phys. Lett 78 (2001) 1367.
[12] Y. Akama, E. Nishimura, A. Sakai, H. Murakami, J. Vac. Sci. Technol. A 8 (1990) 429.
[13] J. Johansson, W. Seifert, V. Zwiller, T. Junno, L. Samuelson, Appl. Surf. Sci. 134 (1998) 47.
[14] T. Bryllert, M. Borgstrom, T. Sass, B. Gustafson, L. Landin, L.-E. Wernersson, W. Seifert, L. Samuelson, Appl. Phys. Lett. 80 (2002) 2681.